J MATER SCI 41 (2006) 4273–4284

Composition and crystal structure of resorbable calcium phosphate thin films

L. TUCK*, M. SAYER
Department of Physics, Queen's University, Kingston Ontario, K7L 3N6, Canada
E-mail: tuckl@physics.queensu.ca

M. MACKENZIE
Department of Physics and Astronomy, University of Glasgow, University Avenue, Glasgow, G12 8QQ, UK

J. HADERMANN
University of Antwerp, Groenenborgerlaan 171, B-2020, Antwerp, Belgium

D. DUNFIELD, A. PIETAK, J. W. REID, A. D. STRATILATOV
Department of Physics, Queen's University, Kingston Ontario, K7L 3N6, Canada

Published online: 15 May 2006

Silicon stabilized tricalcium phosphate (Si-TCP) is formed, among other phases, as a result of sintering hydroxyapatite (HA) in the presence of silica (SiO_2) at >800°C. Calcium phosphate films sintered at 1000°C on quartz substrates are examined with and without additional SiO_2 added to the starting precipitate. Data from transmission electron microscopy (TEM) and X-ray photoelectron spectroscopy (XPS) separate the undoped film morphology into a surface layer with a monoclinic crystal structure $P2_1/a$ characteristic of α or Si-tricalcium phosphate and grain size in the range 100–1000 nm and a substrate layer with a crystal structure which is predominantly apatitic $P6_3/m$ and grain size in the range 30–100 nm. The silicon content is greatest in the substrate layer. The addition of SiO_2 to the film material during fabrication induces a more uniform grain size of 10–110 nm and a higher Si content. The structural and phase evolution of these films suggests the nucleation of α-TCP by the local formation of Si-TCP at a SiO_2-hydroxyapatite interface. The results are consistent with X-ray diffraction studies and are explained by a model of nucleation and growth developed for bulk powders.

1. Introduction

Silicon diffusing from a quartz or silicon substrate into a precipitated calcium hydroxyapatite (HA) coating during firing at 1000°C gives rise to a multiphase system with unique bioactive properties [1, 2]. A combination of material composition and microstructure encourages both osteoclast resorption and osteoblast bone deposition [3, 4]. These materials are commercially available from Millenium Biologix Corp. under the tradename 'Osteologic™' [5]. The commercial materials use undoped hydroxyapatite as the starting precipitate and are fabricated under the same conditions as reported in this paper. The identification of the role of silicon in this process to form a silicon stabilized tricalcium phosphate (Si-TCP) in this multiple phase system has allowed the technology to be transferred from thin films on a quartz substrate to the fabrication of bulk ceramic materials through the addition of silica to a powder precipitate prior to firing [3, 4, 6].

Earlier work on thin films deposited on quartz substrates showed a planar microstructure exhibiting a porous, interconnected morphology with larger surface crystallites, about 1 μm in size [2, 3]. These crystallites are supported on an underlying layer of finer grain material. X-ray fluorescence analysis has shown that the silicon distribution within the film was of highest concentration near the interface with the quartz substrate [2]. From the appearance of the resorption pits arising from osteoclast activity it is apparent that the larger surface crystallites are removed first, with evidence for the underlying substrate layer remaining around the periphery of

*Author to whom all correspondence should be addressed.
0022-2461
DOI: 10.1007/s10853-005-5532-5

the resorption lacunae. The grain size and surface morphology of the film material can be modified by the firing conditions or by the addition of silica to the initial colloidal precipitate [7]. The technology has been applied to Ti6Al4V substrates using a precursor silica layer [8].

In silicon doped bulk powders prepared using the derivative technology, extensive X-ray crystallography has shown that a major component of the multiphase fired material is a type of α-TCP that is stabilized by the presence of silicon [6]. Assuming charge compensation by the formation of OH vacancies, it has been proposed that this material, when fired at temperatures above 800°C has a saturation composition such that 0.33 mol SiO_2 is added to each mol of HA ($Ca_5(OH)(PO_4)_3$), leading to a silicon substituted α-TCP ($Ca_3(P_{0.9}Si_{0.1}O_{3.95})_2$) [7]. This proposed phase, here indicated as Si-TCP_{sat}, is identified using a monoclinic unit cell (with space group $P2_1/a$) similar to the high temperature α-phase of tricalcium phosphate (α-TCP or α-$Ca_3(PO_4)_2$), but with characteristically different lattice parameters. Reid *et al* have previously interpreted crystallographic changes in the overall Si-TCP phase in bulk powders in terms of the co-existence of Si-TCP_{sat} and α-TCP [9]. A model for the reaction chemistry of the multiphase bulk material has been proposed [9].

Several issues in this biomaterial system have not yet been resolved. How the observed phases are nucleated and grown is of interest in understanding the basis for the unique bioactivity of the material system in both bulk and thin film form. A significant empirical finding in the fabrication of bulk material is that the addition of silicon in the form of discrete fumed SiO_2 particles improves the reproducibility of the fabrication process compared with silicon addition via a soluble metal-organic compound [6]. The degree to which an amorphous phase is present has been an uncertainty in the crystallographic analysis of the bulk material [6].

The thin film system has some convenient features for studying both the phase development and the bioactivity of this complex material. The surface structure and morphology are well defined compared to that of the polycrystalline bulk ceramic. In undoped films on quartz substrates, the silicon is provided by unidirectional diffusion from the underlying substrate. In the doped films, silicon diffuses isotropically from particulate SiO_2 located within the film itself as well as from the substrate. Finally, individual particles of the film can be scraped from the substrate and examined by electron microscopy in order to determine the phase composition and crystallography at a local level. This paper demonstrates that many aspects of the undoped films are consistent with properties and reactions of the bulk materials, while doped films behave identically to doped powders. A particular interest is the spatial distribution of silicon within the film with respect to the bulk grains, film surface, film-substrate interface and grain boundaries.

2. Experimental

2.1. Fabrication

Films have been fabricated by a chemical procedure described in previous papers [1, 4]. Ammonium phosphate solution is titrated into an aqueous solution of calcium nitrate adding ammonium hydroxide to keep the pH at 10.5 ± 0.5 according to the following reaction.

$$5Ca(NO_3)_2 + 3NH_4H_2PO_4 + 7NH_4OH \rightarrow Ca_5(OH)(PO_4)_3 + 10NH_4NO_3 + 6H_2O$$

The resulting calcium phosphate solution was then aged at room temperature for 22 h and then concentrated by centrifuge. 1 mm thick fused quartz slides were dipped into the solution. After drying at room temperature, all standard films were sintered at 1000°C for 60 min with a ramp rate of 5°C/min. Films were also prepared from solutions with silica (SiO_2) added using a colloidal suspension of fumed silica (A1695 Cab-o-Sperse™, obtained from the Cabot Corporation, 500 Commerce Dr. Aurora IL 60504) at concentrations of 1 mol SiO_2:1 mol $Ca_5(OH)(PO_4)_3$. The fired films are approximately 1.2 ± 0.2 μm in thickness.

3. Specimen preparation for electron microscopy

Specimens for transmission electron microscopy were prepared by two methods:

1. 3 mm cross sectional discs were created for the TEM by gluing two pieces of quartz together with the films face-to-face in a sandwich structure. These were mechanically thinned and cut to form 3 mm diameter discs. The discs were dimpled from both sides and final thinning was performed by ion milling. The discs were coated with a thin layer of carbon to prevent charging from the electron beam.
2. Thin film powders were prepared by scraping the films from the substrate. The powder was then immersed in methanol, mixed manually, and dispersed using an ultrasonic cleaner for 5 min. A 1000 mesh Soquelec carbon coated copper grid (D20340) was then dipped into the solution to collect the suspended particles.

4. Transmission electron microscopy

Four different microscopes operated in either conventional transmission electron microscopy (TEM) mode and/or scanning transmission electron microscopy (STEM) mode were used in the investigation of the cross sectional thin films and scraped powder particles. Imaging of the cross-sectional samples was performed on a Phillips CM12 and a JEOL 2010F TEM/STEM equipped with a field emission gun at McMaster University. Electron energy loss spectroscopy (EELS) and energy dispersive X-ray (EDX) analysis were undertaken on cross-sectioned

thin films and powders. The amount of calcium, phosphate and silicon present at various points within the samples was determined using EELS data. All EELS spectra were processed to remove multiple scattering and instrumental broadening effects. All other elemental compositions quoted using electron microscopy were the result of EDX. The scraped powder particles were examined at the University of Antwerp using a 400 kV JEOL 400EX microscope (0.17 nm resolution) for taking high resolution images and a 300 kV JEOL 3000F, equipped with an Inca EDX system for making the compositional maps. A Philips CM20 TEM/STEM analytical microscope operated at 200 keV with EDX analytical mapping was also used to collect images and EDX spectra from powder scrapings. Image simulations were made using MacTempas software. EDX measurements of the silicon content of powder, scraped from thin films, using this instrument were calibrated against the silicon content of separately prepared approximately single phase silicon substituted tricalcium phosphate powders doped over a range of 0 – 1.67 wt% Si.

5. X-ray photoelectron spectroscopy (XPS)

XPS was used to quantify Ca, P, Si and O at the film surface. XPS spectra were obtained using a Leybold Max 200 XPS fitted with an Al/Mg X-ray source. Operating conditions during collection were 15 kV and 20 mA using an aluminum anode (Al Kα X-rays). Survey and low resolution spectra were collected from a 4×7 mm^2 area using a pass energy of 192 eV at a take-off angle of 90°. Elemental quantification was obtained from low resolution spectra after a Shirley background removal using relative sensitivity factors (RSF) provided by the manufacturer.

Two independent investigations were performed using XPS. In the first investigation, data was taken after 15 min of argon sputtering to avoid spurious calcium phosphate ratios at the surface of the films. Silicon, calcium, phosphorus and oxygen levels were monitored with respect to sintering time, doping and depth into the surface.

The second investigation was undertaken to examine the effects of different sintering temperatures and times on the surface silicon level and on the calcium phosphate mol ratio (Ca/P) under vacuum. Sintering was done using a Lindberg furnace with a vacuum turbo pump at a pressure of $<10^{-4}$ torr.

6. X-ray powder diffraction (XRD)

X-ray powder diffraction measurements on scraped powders were performed with a Philips X'PERT Pro X-ray diffractometer using Cu–K_α radiation at the line focus of a conventional sealed ceramic diffraction X-ray tube. The working power of the tube was set to 50 kV/30 mA. The incident beam was attenuated with a fixed divergence slit of 1/4°, 0.2 μm solar slits, and a 10 mm incident beam mask. A receiving slit of 0.5 mm and curved graphite monochromator were set in the diffracted beam. Measurements were made using θ–2θ parafocusing Bragg-Brentano geometry with a 2θ step size of 0.02° and a step time of 48 s. The step size was chosen to have five or more steps across the FWHM. Typically, 2θ scans were made from 6–65°. The specimen was set into a depressed quartz plate for analysis using conventional top pack sample loading. 20 – 30 wt% reference material (Si powder-National Institute of Standards and Technology (NIST) SRM #640C or LaB_6 NIST SRM #660a) was added to the film scrapings as a line position standard. Full Pattern Decomposition Fitting using the Le Bail Method [10] was performed on the powder spectra to identify the crystalline phases of the material. In the case of undoped films where the phase composition was known, a Rietveld analysis was carried out using a rigid-body technique [11] to account for the complexity of the α-TCP phase [12]. All analyses were performed using FULLPROF 2000 [13]. These measurements were compared to phase composition measurements using glancing angle XRD which probed the full thickness of an individual film under a procedure described in a previous paper [4].

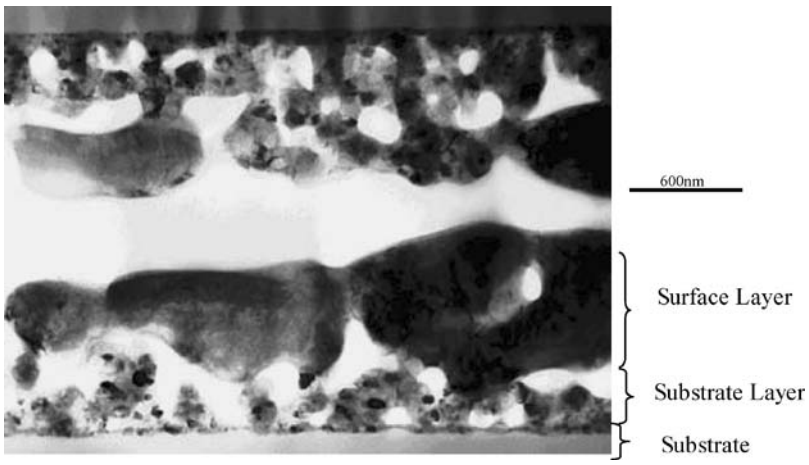

Figure 1 Polished cross-sections of two undoped films glued facing each other. The film morphology can be broken down into the surface and substrate layers.

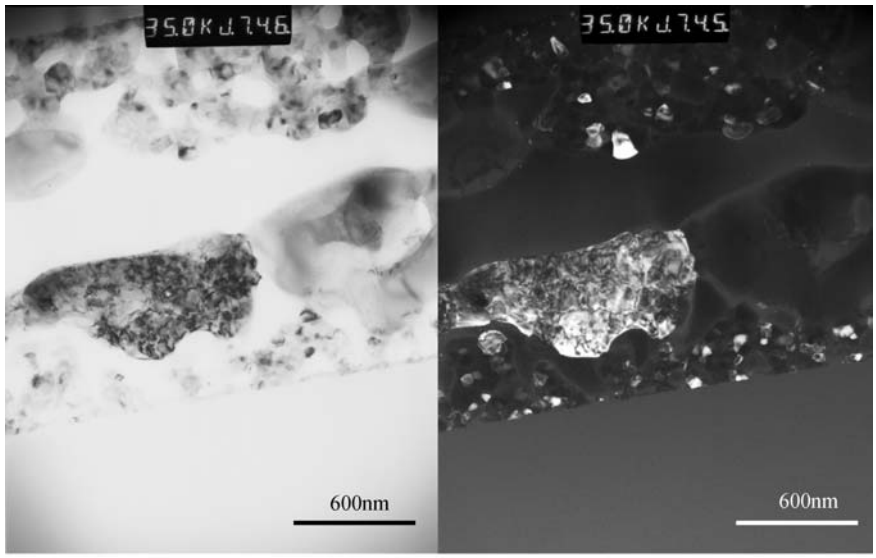

(a)

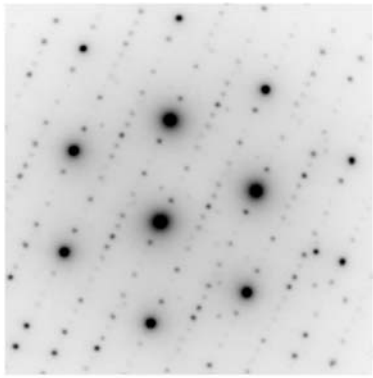

(b)

Figure 2 (a) bright field (b) dark field images of polished cross-sections illustrating the crystallite sizes and orientations in the two layers. (c) A representative diffraction pattern along the [001] zone axis from a large surface crystal. The pattern was indexed to a $P2_1/a$ monoclinic structure and illustrates the pseudohexagonal symmetry characteristic of α- or Si-TCP.

7. Results

7.1. Polished cross-sections of undoped films

7.1.1. Electron microscopy of polished cross-sections of undoped films

The cross-sectional image of a sintered undoped film (containing no additional SiO_2) in Fig. 1 confirms that two distinct layers of crystallites form in the film. A layer of small crystals having a particle size range of 30–100 nm is located adjacent to the substrate surface(substrate layer). Farther from the substrate and forming a second layer adjacent to the first, the crystals are larger in size and range from 100–1000 nm(surface layer). This is consistent with the microporous morphology identified in earlier work [4].

Fig. 2 shows (a) bright field (b) dark field image of a large surface crystal in the polished cross section. It appears to be a large single crystal with a defect structure suggestive of the coalescence of smaller crystallites. A diffraction pattern representative of those taken from various locations in this crystal is shown in Fig. 2c. The [001] zone axis diffraction pattern could be indexed to a monoclinic $P2_1/a$ unit cell consistent with an α- or Si- substituted tricalcium phosphate. The lattice spacings could not be determined with sufficient accuracy to differentiate α-TCP from Si-TCP_{sat} [6]. The crystallinity of the grain is further demonstrated by the high resolution lattice image in Fig. 3. Within the field of view this particle exhibits a single crystal nature with few defects. It is not clear whether the change in the lattice structure at the edge is a real effect or whether it is an artifact of sample preparation or beam damage.

In the layer of crystals close to the substrate, it proved difficult to isolate diffraction patterns from single crystals but polycrystalline ring patterns revealed that the composition was predominantly apatitic with a space group based on $P6_3/m$ unit cell.

8. Chemical analysis of polished cross-sections of undoped films

The chemical compositions at various sites within the two layers of the films are of interest. EELS elemental

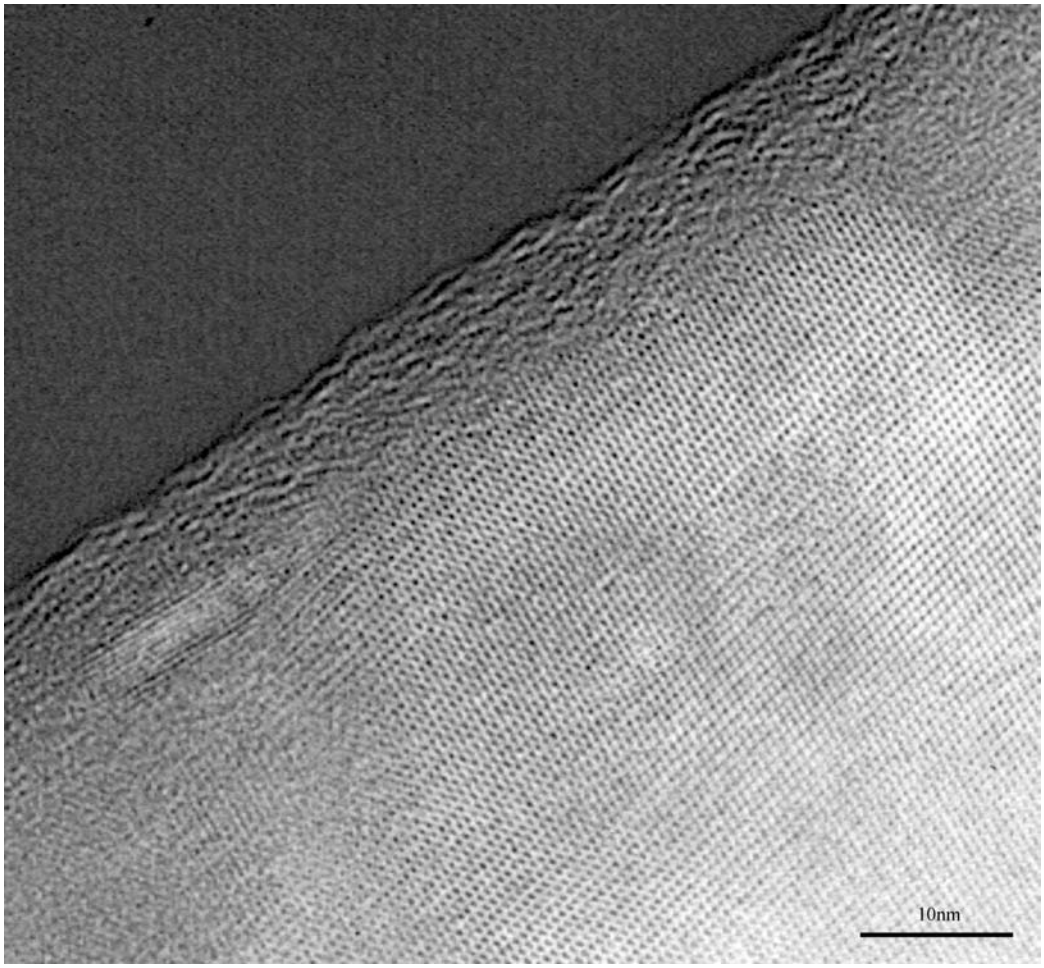

Figure 3 High resolution lattice image from a large surface crystal. This is virtually a single crystal of space group $P2_1/a$, characteristic of α- or Si-TCP, with few structural defects. The surface edge structure may be an artifact of polishing or sample preparation.

compositions determined at 25 different locations within each respecting layer are summarized in Fig. 4a and b for compositions near the substrate (□) and surface (>), respectively. Collection times varied between 5 – 25 s. For samples taken within the substrate layer, the Si content was high and varied greatly, averaging 7 ± 7 at%. The mean Ca/P ratio over the same samples averaged to 1.6 ± 0.2. Samples taken within the surface layer, revealed a lower level of silicon, averaging 2 ± 2 at%. The mean Ca/P ratio was 1.6 ± 0.8. The large variation across these randomly chosen samples would suggest a significant heterogeneity in Si content. Extreme Si contents of 15 – 20 at% and 6 – 7 at% are found in the substrate and surface layers, respectively, of the undoped films. These extreme Si values are found to exhibit low Ca/P ratio's. These extreme values are postulated to be amorphous silica and excluded phosphorus diffusing around the grain boundaries from the substrate. By excluding the extreme data from the calculations, the Ca/P ratio in the substrate and surface layers become 1.6 ± 0.1 and 1.5 ± 0.2 respectively.

9. Electron microscopy of scraped powders

9.1. Undoped films

Given the film morphology of undoped films observed in the previous section and the difficulty of removal of the smaller substrate crystallites during scraping [2], it was anticipated that powders generated from scraped films would primarily consist of the larger surface crystals. Powders generated from scraped films were initially investigated through low magnification (×50 k) TEM. Fig. 5 depicts a piece of scraped film having a porous surface morphology with an average crystallite size of 0.8±0.6 μm. Electron diffraction patterns and high resolution images were taken from a number of individual crystallites in the powders. Representative diffraction patterns along the [001] and [100] zone axes are shown in Fig. 6. All reflections could be indexed using the space group $P2_1/a$ with cell parameters $a = 12.9$ Å, $b = 27.3$ Å, $c = 15.2$ Å, $\beta = 126°$. The uncertainty of measurement was too large to distinguish between α- and Si-TCP_{sat}.

Lattice imaging of the scraped powders complemented these results. Fig. 7 shows a high resolution TEM image along the [100] zone axis. The white dots represent

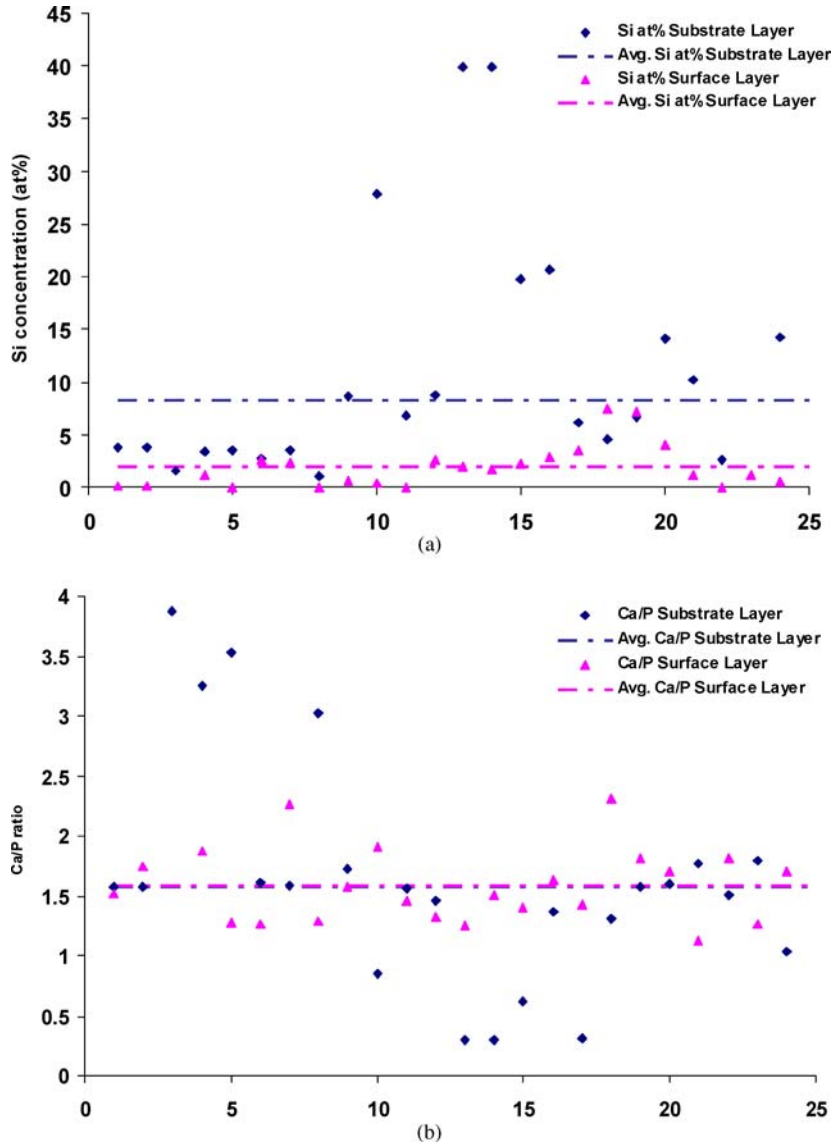

Figure 4 (a) Si concentration (*y*-axis) in the substrate and surface layers with respect to randomly placed sample locations. The *x*-axis number is arbitrary. The concentration and spatial non-uniformity is significantly higher in the substrate layer as well as having a greater mean Si content. (b) Ca/P ratio (*y*-axis) in the substrate and surface layers

the projections of Ca-cation columns. Theoretical simulations of the image along the [100] zone axis using α-TCP cell parameters as input have been superimposed onto the lattice image to show the agreement with the theoretical lattice parameters and structure. A thin white border on the figure outlines the theoretical image. The unit cell is indicated by a denser white rectangle in the corner of the image. The image suggests that the particles in the scraped powder are crystalline to within about 2 nm of the crystal edge and that the existence of amorphous material at the periphery of the grains is difficult to substantiate.

EDX analysis showed that many of the larger crystals derived from the undoped films contained little silicon. Calibration against particles of powders doped with 0–2.16 wt% Si showed that the maximum silicon content was <0.3 wt.%. In these crystals the Si appeared to be homogenously distributed. Examples of EDX maps showing the spatial distribution of silicon in such grains are given in Fig. 8. Fig. 8a and b show single large particles 300–500 nm in size that exhibit homogenously distributed silicon within the single grain yet reveal different Si levels in different particles. Some very Si-rich particles were identified but could not be differentiated from the other particles with imaging or diffraction. However the variability in Si content suggests that particles in different parts of the film experience varying exposure to Si diffusion.

10. Doped films

Fig. 9 shows scraped powders from films prepared from sols of composition 1:1 mol SiO_2: mol HA observed by low magnification (×125 k) TEM imaging. The particle size throughout the doped film is much smaller at 60 ±

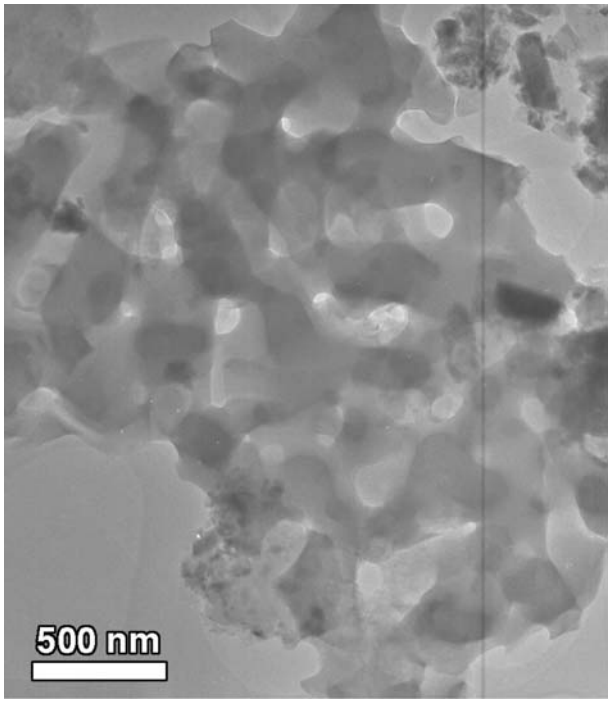

Figure 5 Scraped undoped film fired at 1000°C. Many surface layer granules are observed in an interconnected porous morphology.

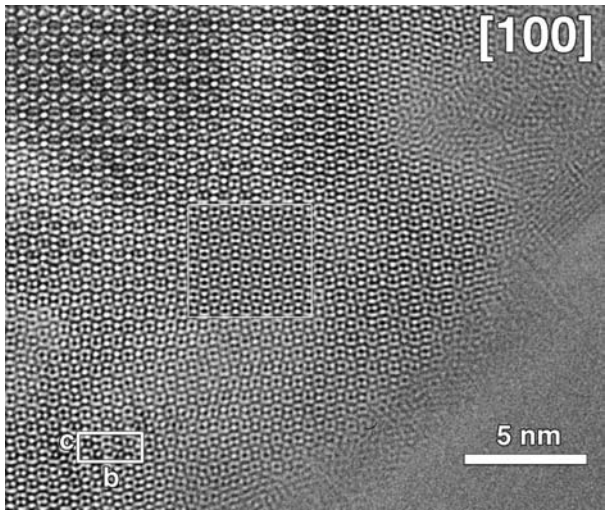

Figure 7 High resolution image of an α- or Si-TCP particle seen along the [100] zone axis. White dots represent the projections of the columns of Ca-cations. The b and c sides of the unit cell are defined within the bold bordered white box while a theoretical lattice image has been superimposed on the image within the thinner bordered white box.

50 nm and the porosity is also reduced. This is consistent with earlier results for films prepared on quartz by rapid thermal annealing [7]. It was difficult to obtain useful electron diffraction patterns from the individual crystals. EDX compositional analysis averaged over many samples revealed a high silicon level with a large variance of 10 ± 7 at%.

11. Surface composition for undoped and doped films

X-ray photoelectron spectroscopy was used to measure the surface composition to a depth of roughly 10–20Å of a film on an underlying quartz substrate over a sampling area of 4×7 mm^2. This technique averages the composition at the surface over many film particles. Measurements of Ca, P, Si and O were made on undoped and doped films for different sintering times and temperatures. For undoped films, Table II lists the concentration of Si and the Ca/P ratio at the surface following a 15 min sintering period at various temperatures to 1000°C. The Si surface composition increased exponentially with temperature to a level of 1.42 at% at 1000°C. This demonstrates the diffusion of Si from the substrate and gives a qualitative measure of the rate of diffusion. The Ca/P ratio remains slightly less than the value of 1.5 expected for stoichiometric α-TCP.

In a separate set of experiments on the effects of sintering time, Fig. 10a shows that the surface Ca/P ratio of undoped films changed from 1.45 to 1.65 while the doped films consistently show a surface Ca/P ratio of >1.67—exceeding the value expected for Si-TCP$_{sat}$. A Ca, P, Si and O profile with respect to depth within the surface was investigated for a 60 min sintered film as a function

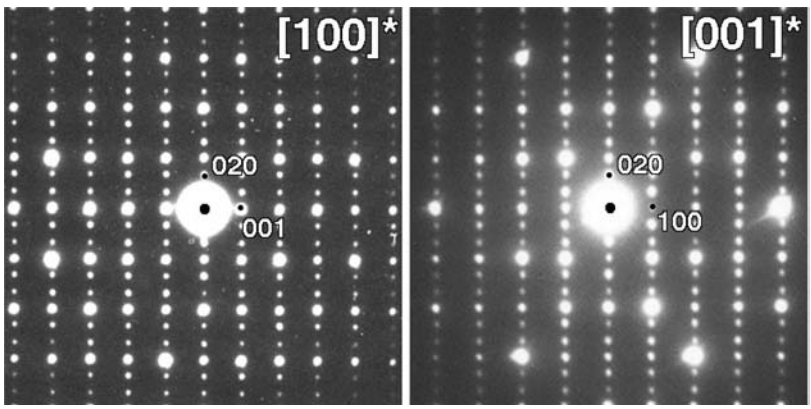

Figure 6 Electron diffraction patterns from surface layer crystals in the [100] and [001] zone axis directions. These patterns fit the P2$_1$/a unit cell with lattice parameters $a = 12.9$ Å, $b = 27.3$ Å, $c = 15.2$ Å, $\beta = 126°$. The uncertainty of measurement cannot distinguish between α- and Si-TCP.

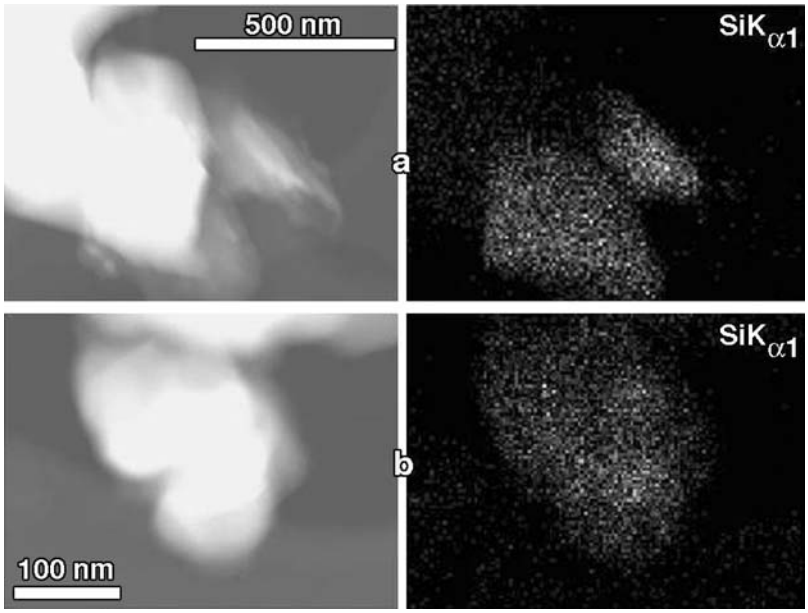

Figure 8 Si elemental maps of (a) homogeneous Si distribution within a large particle of order 500 nm (b) a 100 nm grain with an even Si distribution throughout.

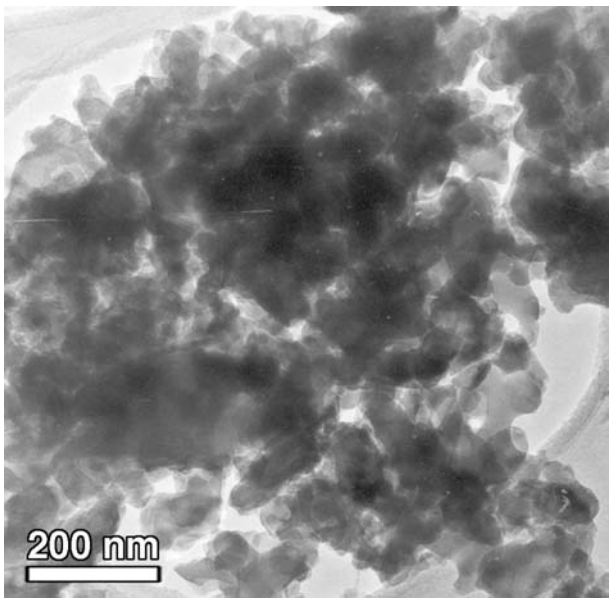

Figure 9 1:1 doped mol SiO_2:mol HA scraped films observed by low magnification imaging. The smaller grain size and reduction of porosity is shown.

of argon sputtering. Each depth unit is 15 min of Ar ion sputtering under the same conditions. Fig. 11 shows that the silicon content is a maximum at the surface while the Ca, P and O contents remained relatively stable. These results suggest that for undoped films sintered for short times, much of the silicon is not included in the TCP crystal lattice but occurs as a superficial surface layer around the grains. However as the sintering time increases, the surface Si content and the Ca/P ratio rises to that expected for Si-TCP$_{sat}$. Films doped with Si during preparation exhibited a surface silicon concentration of up to 10 at% depending on added Si content (Fig. 10b) and a Ca/P ratio of 1.73 (Fig. 10a), both of these quantities changing little with sintering time. This exceeds the theoretical Ca/P ratio for Si-TCP$_{sat}$ of 1.67 indicating perhaps an excess of Ca or a greater deficiency of P.

12. X-ray diffraction

100 slides of films from undoped sols made on quartz substrates sintered for 1 h and 24 h at 1000°C and a doped sol of 1:1 mol SiO_2:mol HA for 1 h at 1000°C were scraped to provide sufficient powder for bulk powder X-ray diffraction. As discussed in Section 3.2, the powder from the undoped films is expected to be primarily representative of the large surface crystallites. The results are summarized in Table I. All errors are calculated using correlated residuals.

Initial studies of powder derived from undoped films used a Rietveld model utilized in earlier studies of powders [6]. For the α-TCP phase this employed an approximation in which three sub cells of the $P2_1/a$ unit cell were averaged. Lattice parameters derived using this model showed that the powder scraped from undoped films conformed to this modified $P2_1/a$ unit cell with lattice parameters a = 12.8796(4) Å, b = 27.3025(3) Å, c = 15.2215(2) Å and β = 126.2225(7)°. These values were compared with lattice parameters published for α-TCP of a = 12.887(2) Å, b = 27.280(4) Å, c = 15.219(2)Å and β = 126.2(1)° [14], and lattice parameters for bulk Si-TCP powders which saturated at a = 12.863(4) Å, b = 27.36(1) Å, c = 15.232(4)Å and β = 126.3(2)° [6]. The comparison suggested that the scraped powder from undoped films had lattice parameters closest to α-TCP.

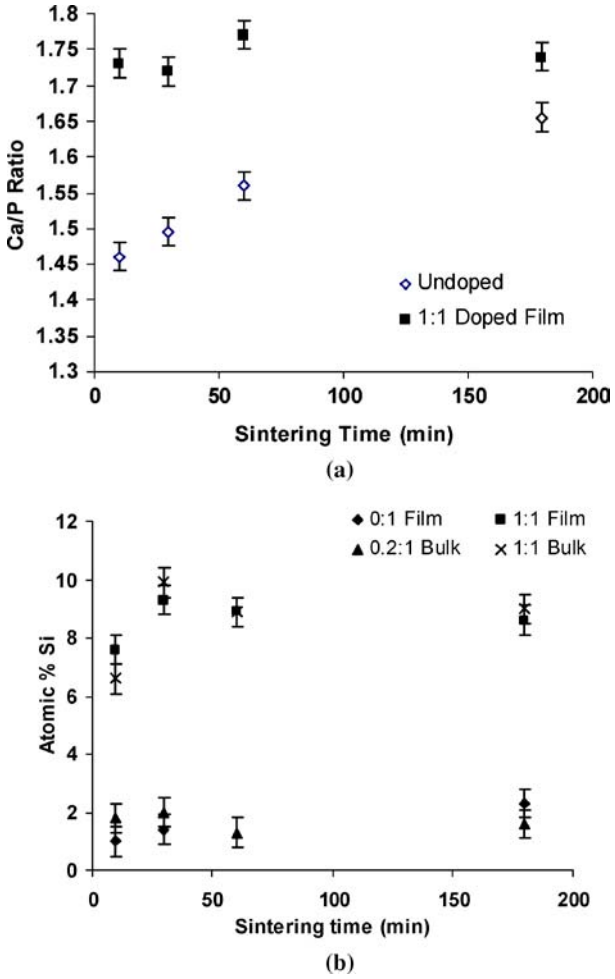

Figure 10 (a) The Ca/P ratio of undoped films measured by XPS increases from a value of ∼1.5 (α-TCP) to 1.7 (Si-TCP) as sintering time increases. Doped films exhibit a consistent value of ∼1.7 (b) XPS measurements of Si after being sputtered by argon gas for 15 min.

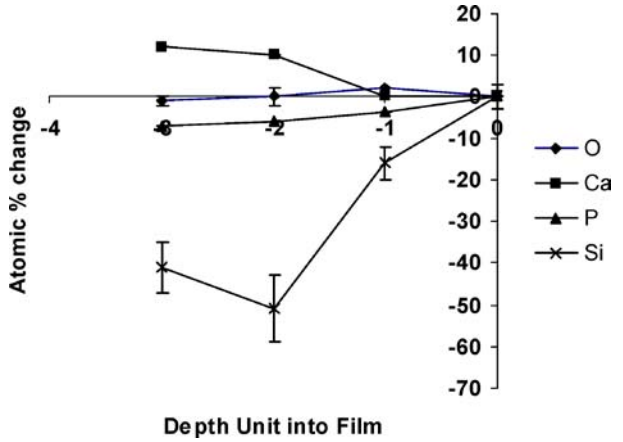

Figure 11 Change in atom concentration as a function of depth for an undoped film by XPS measurements of Si, Ca, P and O after sputtered by argon gas. The depth unit is relative corresponding to 15 min sputtering time under similar conditions.

In a separate Le Bail analysis, which included a Si standard in the original data acquisition, the data was evaluated on the basis of the full $P2_1/a$ unit cell [12]. An refined spectra is shown in Fig. 12a and b to demonstrate the quality of fit. Both this and a Rietveld fit based on a full unit cell of the same data showed that the undoped powder consisted of a single phase with $P2_1/a$ symmetry and lattice parameters [15, 16], $a = 12.891(9)$Å, $b = 27.3073(1)$Å, $c = 15.226(4)$Å, $\beta = 126.24(1)^\circ$. The a-axis parameters match the value for α-TCP while the b and c-axis lattice parameters fall in between the cited parameters for α- and Si-TCP_{sat}.

By contrast, glancing angle diffraction spectra taken on an individual undoped film and therefore representative of all phases present greater than 5%. These showed that the phase composition ranged between 67 – 75% α- or Si-TCP ($P2_1/a$) and 25 – 33% HA ($P6_3/m$) [3]. Taken in conjunction with the TEM results in Section 3.1, this implies that the HA primarily resides in the substrate layer and is not detached by scraping. This finding is consistent with the Ca/P ratio of 1.6 ± 0.8 in the substrate layer discussed earlier.

Further studies were made of a powder derived from undoped films and sintered for 24 h. A Le Bail fit revealed a $P2_1/a$ unit cell with lattice parameters $a = 12.8998(4)$Å, $b = 27.2979(8)$Å and $c = 15.2155(3)$Å and $\beta = 126.236(2)^\circ$. These values conform to α-TCP with the exception of the b-axis which falls in between the cited lattice parameters for α- and Si-TCP.

Le Bail analysis of the X-ray diffraction data taken on doped 1:1 mol SiO_2:mol HA films with a LaB_6 standard showed a multiphase system consisting of TCP and apatite phases having $P2_1/a$ and hexagonal $P6_3/m$ symmetry, respectively. The refined lattice parameters are $a = 12.868(6)$Å, $b = 27.3202(1)$Å and $c = 15.238(3)$Å, $\beta = 126.04(1)^\circ$ and $a = 9.4081(1)$Å, and $c = 6.8861(1)$Å for the respective symmetries and phases. The a- and c-axis parameters conform closely to those of Si-TCP, with the largest discrepancy again being for b-axis, which falls in between the values for α- and Si-TCP. By comparison with the work of Bonfield, the apatite phase lattice constants match that of silicon-substituted apatite, similar in structure to HA [17].

13. Discussion

Cross-sectioned films provide detailed information on the phase morphology of the undoped sintered films with little uncertainty about the location of the sample under examination. Two clear regions exist within the ∼1 μm thick layer of the undoped film. Smaller crystallites reside near the substrate and are mainly composed of an apatite phase. Electron diffraction data shows that this region contains a mixture of hexagonal structured $P6_3/m$ apatite and trace amounts of monoclinic $P2_1/a$ phase. The surface layer tends to larger single crystal grains of a monoclinic $P2_1/a$ structure formed on the smaller crystallites below it.

Powders derived from scraped undoped films showed large crystallites (0.1–1.3 μm diameter crystals) with a

TABLE I Lattice parameters obtained using Le Bail and Rietveld analysis of XRD spectra. All errors are calculated using correlated residuals

Sample	Refinement Method	a (Å)	b (Å)	c (Å)	β (°)
α-TCP	Mathews *et al*. [14]	12.887(2)	27.280(4)	15.219(2)	126.2(1)
Si-TCP	Rietveld, 1/3 unit cell [6]	12.863(4)	27.36(1)	15.232(4)	126.3(2)
Undoped film, 1 h @ 1000°C	Rietveld, 1/3 unit cell	12.8796(4)	9.10084(8)	15.2215(2)	126.2225(7)
Undoped film, 1 h @ 1000°C	Rietveld, full unit cell [16]	12.881(4)	27.30218(5)	15.222(2)	126.22(1)
Undoped film, 1 h @ 1000°C	Le Bail, full unit cell	12.891(9)	27.3073(1)	15.226(4)	126.24(1)
Undoped film, 24 h @ 1000°C	Le Bail, full unit cell	12.8898(4)	27.2979(8)	15.2155(3)	126.236(2)
1:1 doped film, 1 h @ 1000°C	Le Bail, full unit cell	12.867(6)	27.3202(1)	15.238(3)	126.06(1)

TABLE II Si surface concentration and Ca/P ratios at the surface of undoped films after a 15 min sintering period at various sintering temperatures under vacuum

Temp	Unsintered	200°C	400°C	700°C	1000°C
at% Si	0.00 at%	0.02 at%	0.10 at%	0.19 at%	1.42 at%
Ca/P	1.47	1.48	1.42	1.46	1.39

monoclinic $P2_1/a$ structure characteristic of crystallites found at the surface of the cross-sectioned film. The surprising result from Rietveld and Le Bail XRD refinement revealed that the surface crystals conform more closely to an α-TCP rather than a Si-TCP phase. α-TCP has been considered a high temperature TCP phase (>1175°C), with β-TCP existing at room temperature in ambient conditions [14], although recent work has shown that α-TCP can be produced at lower temperatures (~650°C) from an amorphous precursor [18].

Surface Ca/P ratios and Si levels range from 1.4–1.7 and 0.0–1.2 at% respectively with sintering time implying a surface phase change from α- to Si-TCP on undoped films. EDX observations reveal higher concentrations of Si close to the substrate and finds silicon throughout the surface layer. This is thought be Si that is on the grain boundary or crystal surface perpendicular to the beam that was not removed by the ion beam during milling and is therefore not substituted in the crystal.

Doped films have a single layer composed of smaller crystallites throughout the film. Chemical and diffraction measurements show a high bulk and surface silicon content as shown in Fig. 10b, a Ca/P ratio >1.67 shown in Fig. 10a, and unit cell lattice parameters most characteristic of Si-TCP_{sat}.

The difference during the firing of undoped and doped films is the direction of movement and availability of the source of silicon. In the undoped film this occurs because of the directional diffusion of Si from the underlying substrate. In doped films, isotropic diffusion around the SiO_2 particles included in the precipitate adds to and dominates the diffusion of Si from the substrate depending on sintering time and temperature. The effects of SiO_2 particles pinning grain boundaries in films during crystal growth previously described by Pietak *et al*. [7] is reproduced in the present work. Significant migration of Si to the film surface occurs for doped films.

In bulk powders, Si-TCP_{sat} is stable above 800°C [7] in normal atmospheric conditions. Reid *et al*. [10] have proposed a two stage process leading to the formation of Si-TCP_{sat} having composition $Ca_3(P_{0.9}Si_{0.1}O_{3.95})_2$.

$$Ca_5(PO_4)_3OH + BSiO_2 \rightarrow CCa_5(PO_4)_{3-x}(SiO_4)_X (OH)_{1-X} + DCa_3(PO_4)_2 + EH_2O$$

$$Ca_3(PO_4)_2 + (0.2 + \Delta B)SiO2 \rightarrow Ca_3(P_{0.9}Si_{0.1}O_{3.95})_2 + 0.1\,P_2O_5 \cdot \Delta BSiO_{2(amorphous)}$$

The initial effect of SiO_2 on the HA precipitate during firing is to form a silicon substituted dehydrated apatite (*C* phase) and α-TCP (*D* phase). In the continuing presence of SiO_2 the α-TCP lattice will take up to 0.33:1 mol SiO_2:mol HA to form Si-TCP_{sat} with the remaining SiO_2 being excluded from the lattice along with the phosphorous from the substitution sites in an amorphous material. In the undoped film with its limited supply of Si, the experimental evidence suggests that crystals of the α-TCP phase will grow as soon as some Si-TCP nuclei are formed. Coalescence of these crystals then appears to limit the diffusion of Si into their bulk, although it appears from the average Si surface content equivalent to 0.33:1 mol SiO_2:mol HA (1.5 at%) that a thin surface layer of Si-TCP_{sat} may form relatively easily, with the final surface concentration being set by the saturation SiO_2 content and sintering conditions. In doped films, the supply of SiO_2 is sufficient not only to fully create Si-TCP_{sat}, but that subsequent diffusion and the exclusion of Si predicted by the chemical model creates large Si concentrations on the surface of the crystals. Other factors may also be operating.

The lattice constants for powders from both the 1 h and 24 h undoped sol scrapings were closest to those of the α-TCP phase. The presence of α-TCP in undoped films can be explained in terms of the rapid agglomeration and growth of small grains during sintering into large single crystals. As per the model for the formation of Si-TCP in bulk ceramics [19], silicon diffusion from the quartz substrate nucleates silicon apatite (Si-Ap) and α-TCP in the calcium phosphate film in the substrate layer region directly adjacent the substrate. While the silicon acts to pin the grain boundaries in the substrate layer resulting in small grains, as observed during this work and by Pietak *et al* [7] for doped films, the α-TCP phase propagates epitaxially straight through the thickness of the film with only

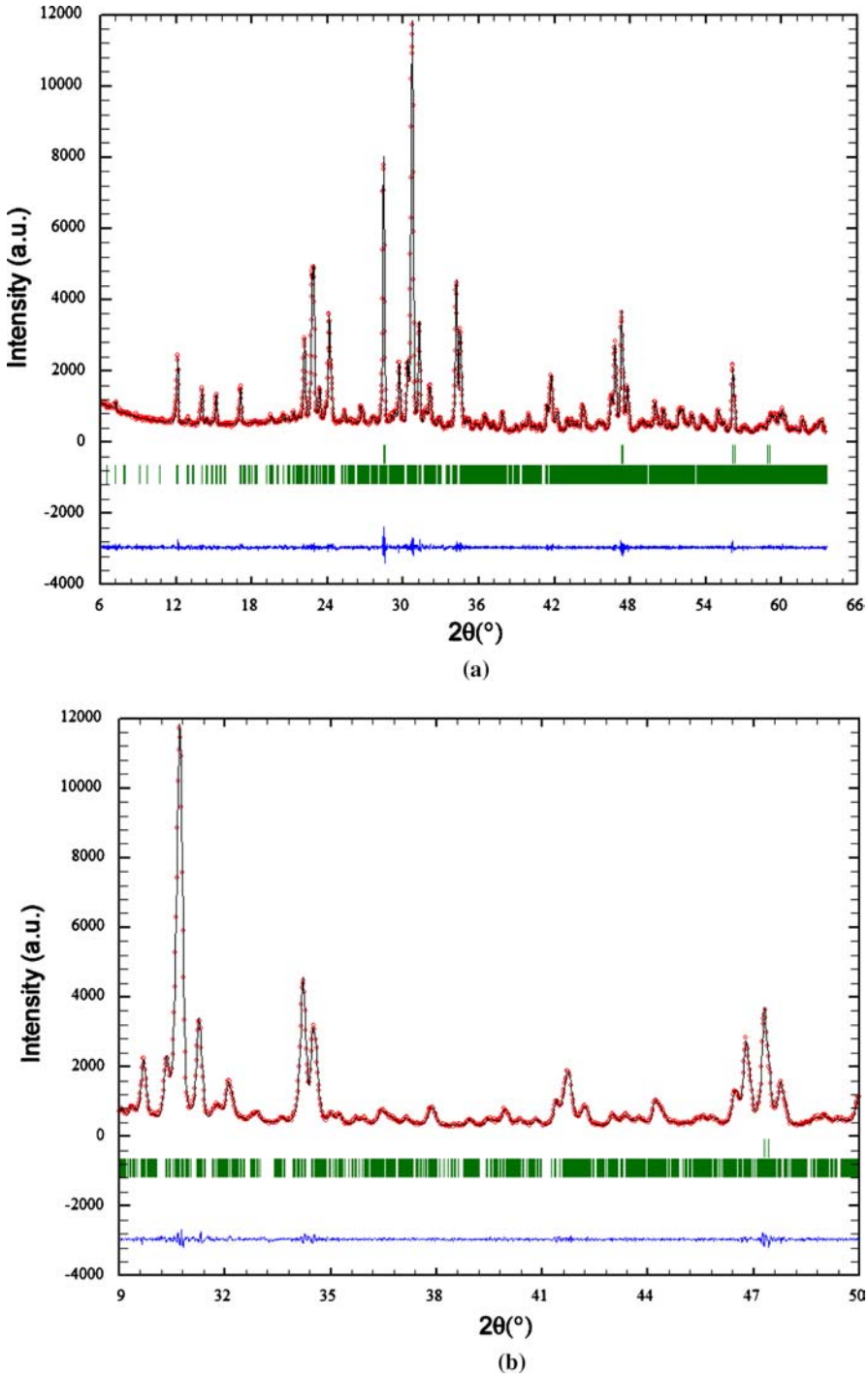

Figure 12 (a) Le Bail profile analysis for powders scraped from undoped films with a Si powder internal standard. (b) Demonstration of the quality of fit for the undoped film over a restricted range of 2θ.

small amounts of Si substitution of the phosphorus sites creating a low level Si-TCP. In the absence of sufficient silicon to pin the grain boundaries of these low doped Si-TCP grains, they agglomerate and form large, predominantly single crystal α-TCP in the surface layer. Over time Si may slowly be removed from the TCP lattice and is displaced to the grain surface. This process and the diffusion of substrate silica up the grain boundaries, surrounds the α-TCP crystals and accumulates with time at the film surface, as demonstrated by various measurements including XPS, EDX and EELS. Silicon encapsulation of the surface crystals and at grain boundaries may act to stabilize the α-TCP phase indefinitely by forming a thin layer of Si-TCP_{sat} or silica, on the order of angstroms, around the inner α-TCP core. The size of the surface crystals, and their inherent propensity to minimize their interfacial surface free energy, may also aid the stability of the α-TCP phase.

Recent ab-initio calculations of the energy of Si substituting in various calcium phosphate lattices suggests that the energy of Si in an α-TCP lattice is much higher than in an HA lattice [19]. Si diffusing from the substrate may segregate into the apatite formed in the substrate layer at the expense of diffusion towards the surface.

The consequence of these results for the interpretation of the biological activity of 'Osteologic^{TM}' slides is of interest. The first observation is that bioactivity is higher for undoped films and lower for doped films having a starting composition of 1:1 mol SiO_2:mol HA. This appears to be closely linked to the surface silicon content where osteoclast bioactivity is minimized above a particular value. It may be that the rapid formation of Si-TCP_{sat} at its saturated composition through the chemical model noted above, plays an important role in fixing this concentration at 1.5 at% (0.33:1 mol SiO_2:mol HA). Pietak *et al* have recently shown that protein adsorption on bioceramic surfaces can be influenced by surface silicon [20].

14. Conclusions

The structure of undoped and SiO_2 doped hydroxyapatite thin films sintered on quartz substrates is strongly influenced by the directional nature of silicon diffusion. A silicon stabilized tricalcium phosphate phase, with a $P2_1/a$ crystal structure, initially formed at a SiO_2-hydroxyapaptite interface can then nucleate the growth of an undoped α-TCP phase in adjoining regions of the film. In undoped films the rate of unidirectional Si diffusion from the substrate is lower than the rate of propagation of the crystallization front, resulting in a low Si-TCP concentration in large crystals formed away from the substrate region. When SiO_2 particulates are distributed throughout the precipitate prior to firing, these conditions are not met and the smaller grained structure is predominantly Si-TCP. The microstructure does not indicate that a substantially distinct amorphous or glassy phase is present in isolated regions, but that a superficial surface layer of composition set by the formation of silicon stabilized tricalcium phosphate (Si-TCP_{sat}) may occur on the exterior of larger surface crystallites. This may play an important role in determining the bioactivity of these thin film bioceramics. The structure and phase composition of the films is consistent with a model developed for multiphase Si doped TCP ceramic powders with both α- and Si-TCP phases existing in the system.

Acknowledgements

Financial support from Millenium Biologix Corp. and the Natural Sciences and Engineering Research Council is acknowledged. Assistance in analytical work by Jo Verbeeck at the University of Antwerp is appreciated. The authors would like to thank Andy Duft (McMaster University) for preparation of cross-sectional TEM specimens.

References

1. Q. QUI, P. VINCENT, B. LOWENBERG, M. SAYER and J. E. DAVIES, *Cells Mater* **3**(4) (1993) 351.
2. S. LANGSTAFF, M. SAYER, L. WEAVER, S. PUGH and T. J. N. SMITH, *Mat. Res. Soc. Proc.* **414** (1996) 87.
3. S. LANGSTAFF, M. SAYER, T. J. N. SMITH, S. M. PUGH, S. A. M. HESP and W. T. THOMPSON, *Biomaterials.* **20** (1999) 1727.
4. S. LANGSTAFF, M. SAYER, T. J. N. SMITH and S. M. PUGH, *Biomaterials.* **22** (2001) 135.
5. Millenium Biologix Inc, 785 Midpark Drive, Kingston, Ontario, Canada. K7M 7G3.
6. M. SAYER, A. D. STRATILATOV, J. REID, L. CALDRIN, M. J. STOTT, X. YIN, M. MACKENZIE, T. J. N. SMITH, J. A. HENDRY and S. D. LANGSTAFF, *Biomaterials.* **24** (2003) 369.
7. A. PIETAK, M. SAYER and M. J. STOTT, *J. Mater. Sci.* **39** (2004) 1.
8. J. REID, M. SAYER and T. J. N. SMITH, *Mat. Res. Soc. Symp. Proc.* **717** (2002) 11.
9. J. REID, A. PIETAK, M. SAYER, D. DUNFIELD and T. J. N. SMITH, *Biomaterials* (2004) (in press).
10. A. LE BAIL, H. DUROY and J. L. FOURQUET, *Mat. Res. Bull.* **23** (1988) 447.
11. V. RODRIGUEZ, and J. RODRIGUEZ-CARVAJAL, *J. Applied Cryst.* (to be published).
12. D. DUNFIELD, *J. Applied Cryst.* (in preparation).
13. FULLPROF 2000, Rodríguez-Carvajal J, Laboratoire Léon Brillouin (CEA-CNRS) CEA/Saclay, 91191 Gif sur Yvette Cedex, France.
14. M. MATTHEW, L. SCHROEDER, B. DICKENS and W. E. BROWN, *Acta Cryst.* **B33** (1977) 1325.
15. Errors were calculated using correlated residuals: J. F. BERAR and P. LELANN, *Appl. Cryst.* **24** (1991) 1; J. F. BERAR, "Acc. in Pow. Diff. II." *NIST Sp. Pub.* **846** (1992) 63.
16. D. DUNFIELD, L. CALDRIN, M. J. STOTT and M. SAYER, in "The powder refinementof α-tricalcium phosphate Ca3(PO4)2" (in preparation).
17. R. GIBSON, S. M. BEST and W. BONFIELD, *J. Biomed. Mater. Res.* **44** (1999) 422.
18. TAKAFUMI, T. UMEGAKI and N. UCHIYAMA, *J. Chem. Tech. Biotechnol.* **32** (1982) 399.
19. Personal Communication with Dr. M. Stott, Queen's University (2005).
20. PIETAK, D. SINDREY, M. SAYER and M.J. STOTT, in "The Bioactive Effects of Aqueous Silicate Introduced to Extracellular Media by Skelite Materials" (to be published).

Received 17 June 2004
and accepted 15 July 2005